RESULTS & DISCUSSION

Chapter 3

RESULTS AND DISCUSSION

3.1 Thermodynamic clarifications for combustion synthesis of TiC/Al_2O_3

3.1.1. Effect of initial temperature on the adiabatic temperature

The adiabatic temperature T_{ad} of combustion reaction is the maximum achievable combustion temperature in case of adiabatic conditions (no energy loss from the reaction medium). It depends mainly on the initial temperature of the reaction. It is directly proportional to the enthalpy of the reaction ΔH_r and the initial temperature T_o and inversely proportional to the specific heat capacity of system C_p. The adiabatic combustion temperature can be calculated at any initial temperature T_o from the following general equation:

$$-\Delta H_{r,\,To} = \int_{To}^{Tad} C_p\,(\text{product})\,dT$$

Where, Cp in its general form is represented as:

$$Cp = A + B\,10^{-3}\,T + C\,10^{5}\,T^{-2} + D\,10^{8}\,T^{-3} \quad Jmol^{-1}K^{-1}$$

A, B, C and D are the heat capacity constants of the products which are specific and unique for each material according to the equation:

$$TiO_2 + C + 4/3\ Al \longrightarrow TiC + 2/3\ Al_2O_3 \quad , \Delta H = -358.443\ K\ J/mol$$

In case of TiC/Al_2O_3 the values of these constant are as follows:

A = 126.441, B = 9.498, C = -38.409, D = 1.887. [121]

Integration of this general equation and rearrangement of the results give the following equation:

$$B\,T^2_o\,T^4_{ad} + 2\,A\,10^3\,T^2_o\,T^3_{ad} + [10^{11}\,D + 2\,C\,10^8\,T_o - 2\,A\,10^3\,T^3_o - B\,T^4_o + T^2_o\,(\Delta H_{To} - \mu\Delta H_{f,\,Al2O3})]\,T^2_{ad} - 2\,C\,10^8\,T_o\,T_{ad} - 10^{11}\,D\,T^2_o = 0$$

Where, μ is the fraction of molten Al_2O_3 and $\Delta H_{f, Al2O3}$ is the enthalpy of fusion of Al_2O_3 (112.99 kJ/mol).

So at any given initial temperature T_o, substitution in the above equation by the values of *A, B, C, D,* and *ΔH* of the reaction yields the corresponding adiabatic temperature T_{ad}. Fig. 8 represents the calculated adiabatic temperature of the combustion synthesis of TiC/Al_2O_3 from TiO_2, Al and C at different initial temperatures. It can be seen that the adiabatic temperature of the reaction at 298 K is 2403 K which is higher than that of the melting point of Al_2O_3 (2323 K) and lower than that of TiC (3100 K) [119]. This value of T_{ad} is higher than that of the empirical value 1800 K which means that the reaction between TiO_2, Al and C can proceed in a self-sustaining manner. Also, the adiabatic temperature of the reaction increases linearly with increasing the initial temperature. The noticed linear relation between T_{ad} and T_o is due to the stepwise accumulation of energy with increasing the initial temperature which raises the total energy of the system which in turn leads to a higher combustion temperature.

3.1.2. Effect of aluminum additions on the adiabatic temperature

$$TiO_2 + C + (4/3 + x)\,Al \longrightarrow TiC + 2/3\,Al_2O_3 + x\,Al,$$

$$\Delta H = -358.4 \text{ kJ/mol}$$

where, *x* is the amount of excess aluminum per one mole of TiC.

The enthalpy of fusion of Al $\Delta H_{f,Al}$ (10.7 kJ/mol) should be subtracted from the general equation as follows:

$$B\,T^2_o\,T^4_{ad} + 2\,A\,10^3\,T^2_o\,T^3_{ad} + [10^{11}\,D + 2\,C\,10^8\,T_o - 2\,A\,10^3\,T^3_o - B\,T^4_o + T^2_o\,(\Delta H_{To} - \mu\Delta H_{f, Al2O3} - x\Delta H_{f,Al})]\,T^2_{ad} - 2\,C\,10^8\,T_o\,T_{ad} - 10^{11}\,D\,T^2_o = 0$$

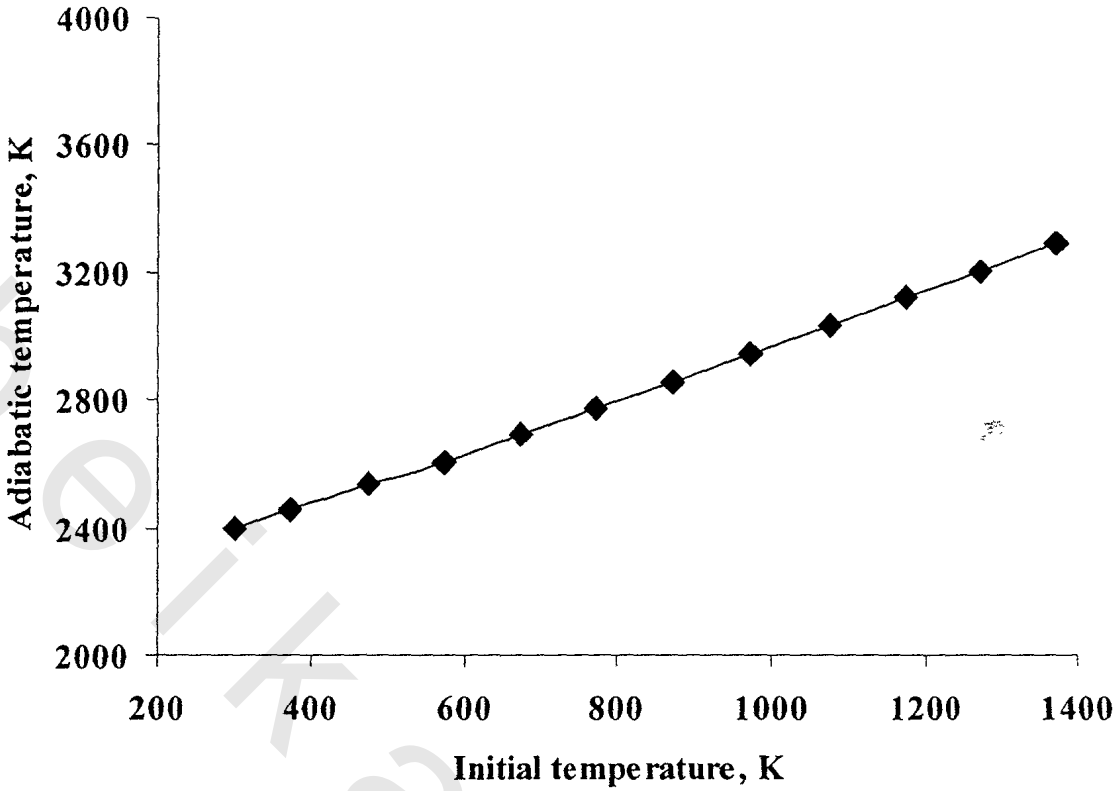

Fig. 8 Dependence of adiabatic temperature of TiC/Al_2O_3 on the initial temperature of the reactants

Fig. 9 shows the effect of excess Al on the T_{ad} of the combustion reaction at 298 K. Increasing value of x to 0.159 reduces T_{ad} to the melting point of Al_2O_3 (2323 K) and then T_{ad} becomes constant at this value over a wide range of excess Al from x = 0.159 to x = 1.164 during the phase transformation of the produced Al_2O_3 into liquid phase and then decreased again with further Al additions. Further Al additions beyond 1.164 mol led to a stepwise decrease in the value of T_{ad}.

This behavior can be explained as follows: at 298 K and where no excess Al, the calculated T_{ad} is 2403 K which means that the entire amount of Al_2O_3 in the product is in the molten state. Excess Al does not participate in the reaction and it works as inert phase (diluents) which absorbs some of the energy liberated from the combustion reaction and undergoes physical change from solid to liquid phase. This brings about drop in the amount of energy and the calculated T_{ad} is gradually reduced from 2403 to 2323 K with increasing the amount of excess Al to x = 0.159. At x = 0.159, the entire amount of Al_2O_3 is in the molten state. The stability of the calculated T_{ad} at 2323 (m.p. of Al_2O_3) with increasing the extra amount of Al to < 1.164 mol is due to the presence of some fraction of molten Al_2O_3 in product as shown in Fig. 10. At $x \geq 1.164$, the entire amount of Al_2O_3 changed into solid phase, so the T_{ad} starts to decrease again.

On the other hand, the dependence of the molten fraction of Al_2O_3 on the amount of excess Al is given in Fig. 10. At $x \leq 0.159$, the calculations show that 100 % of Al_2O_3 is in the molten state. However, at $x > 0.159$, fraction of molten Al_2O_3 gradually decreases and become zero at $x \geq 1.164$.

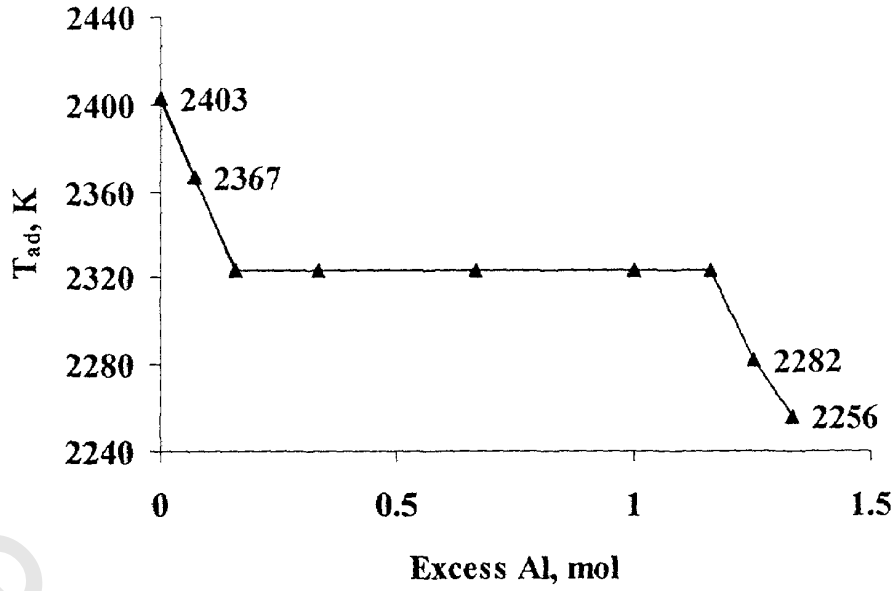

Fig. 9 Effect of excess Al on the adiabatic temperature for (TiO_2 + (4/3+ x) Al + C) reaction

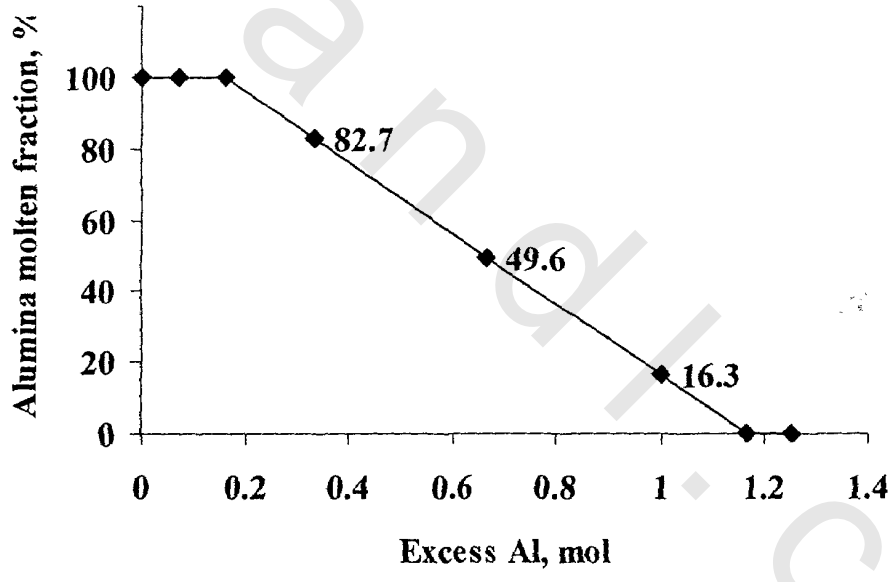

Fig. 10 Effect of excess Al on the molten fraction of Alumina for (TiO_2 + (4/3+ x) Al + C) reaction

3.2 Synthesis of titanium carbide/aluminum oxide composite by self-propagating combustion technique (SHS)

The raw materials powders TiO_2 (<1 μm), Al (≤93 μm) and C (~78 μm) are weighed in the required ratio for the preparation of TiC/Al_2O_3 composite. These powders are then mixed and pressed yielding green compacts from 53 to 55 % relative density. The combustion synthesis is investigated under argon atmosphere, at different grain sizes and molar ratios of aluminum powder (< 20 μm: 72 μm) and (1 mole: 6 moles) respectively. The effect of preheating the green compacts up to 597 °C is also studied. The temperature profile of each experiment is recorded using the previously described type C thermocouple.

3.2.1 Synthesis of TiC/Al_2O_3 composite at room temperature

Combustion synthesis of TiC/Al_2O_3 composite is carried out under argon atmosphere using (TiO_2, Al and C) mixture having stoichiometric ratio of 3:4:3 at room temperature, where, the grain size of aluminum powder is less than 36 μm. The temperature profile of the combustion synthesis of TiC/Al_2O_3 from its raw materials is shown in Fig. 11. It consists of two temperature profiles one for the upper thermocouple (I) near igniter and the other for the second thermocouple (II) about 1 cm down from the upper one.

Generally, the temperature profiles show an abrupt rise in temperature as the wave passes in the location of the embedded thermocouple and then the temperature decreases dramatically due to heat losses. Although, this reaction is carried out at room temperature, the initial temperature of the compact is shifted to a higher value due to the heat supplied from the igniter.

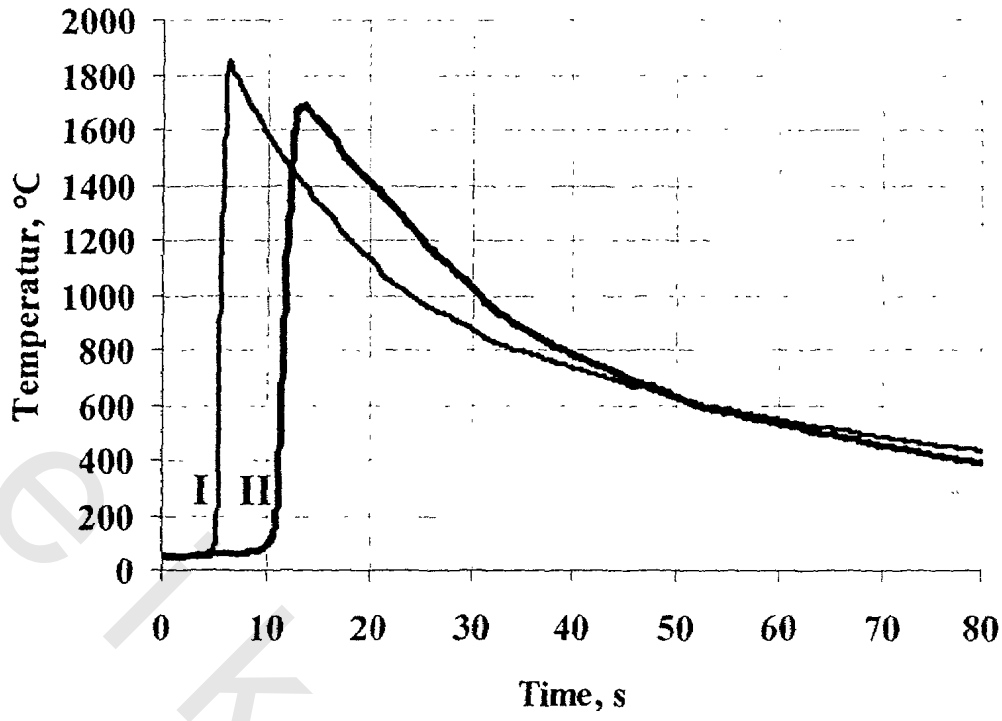

Fig. 11 Temperature profiles from the upper and lower locations of the $3TiO_2+4Al+3C$ reaction carried out at room temperature (initial)

The initial temperature of the upper location (upper thermocouple I) is raised from room temperature to 73 °C while the lower location (lower thermocouple II) shows a temperature of 56 °C. It is worth to mentioning that the onset temperature of the specimen strongly affects the temperature profile as well as the wave velocity. So, a great care is taken in order to determine the actual initial temperature (*onset*) of the profile which is not necessarily the starting one. The temperature profile of the upper thermocouple has a maximum at 1857 °C with temperature rise of 1784 °C, reached after 1.4 s. and recorded by the data acquisition system. On the other hand, the profile of the lower thermocouple has a maximum temperature of 1692 °C with temperature rise of 1636 °C within 2.9 s. The adiabatic temperature of the reaction between reactants as well as the rate of heating *(dT/dt)* is calculated using the methods previously reported. [19] When the onset temperatures are 73 °C and 56 °C, the adiabatic temperatures are 2162°C and 2151°C respectively, which are below the melting point of titanium carbide (3100 °C) and higher than that of aluminum oxide(2053°C). [119]

The first derivatives of the temperature profiles, *dT/dt* (rate of heating), of the upper and lower locations, Fig. 12, (A and B), reveals that maximum heating rate during the combustion synthesis is 3464 °C s^{-1} and 1347 °C s^{-1} respectively.

The wave velocity calculated from monitoring the time difference between the two peaks of the temperature profiles is relatively low and equals 1.56 mm/s. This is in consistent with the observed wave behavior of the reaction, which is a non-steady state (pulsating planer) as in Fig. 13.

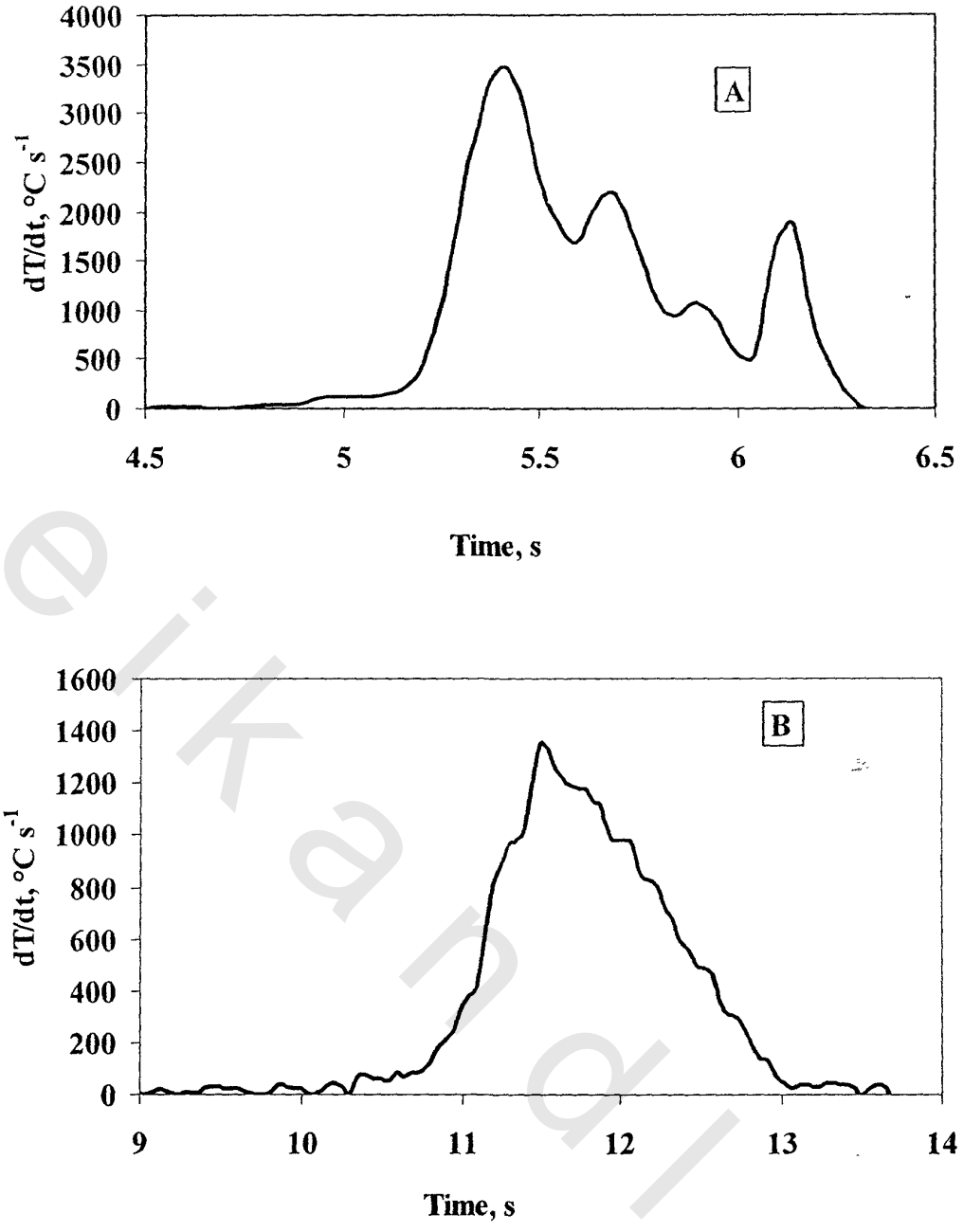

Fig. 12 First derivatives of the temperature profiles of $3TiO_2+4Al+3C$ reaction carried out at room temperature:

A) Upper location, 73 °C (*onset*);

B) Lower location, 56 °C (*onset*)

3.2.2 X-ray diffraction pattern (XRD)

X-ray diffraction pattern of this specimen after combustion, Fig. 14, reveals the existence of very sharp lines corresponding to the diffraction pattern of titanium carbide and aluminum oxide. No elemental powders are detected; this suggests that the reaction between TiO_2, Al and C has very high degree of conversion at these conditions.

3.2.3 Microstructure investigations

3.2.3.1 Optical microscopy (OM)

The microstructure of the SHS product TiC/Al_2O_3 (longitudinal section) is shown in Fig.15. Fig. 15a shows the formation of laminated structure of alternatively pores and ceramic, this proves that the reaction occurs in pulsating mode where the combustion wave travels in a planer but pulsating manner. On the other hand, Fig.15b (higher magnification) shows the presence of different types of porosity, colorless phase and dark phase.

The morphology of the porosity has been shown to exist in two major forms, long radial pores and small micropores. The volume fraction of the pores is measured by Archimedean method and equals to 43 %. The appearance of these pores is thought to be mainly due to the initial green body porosity 47 %, outgassing of adsorbed gases during the high temperature reaction and the densities difference between the reactants and products, (3347 kg m^{-3}) and (4360 kg m^{-3}) respectively.

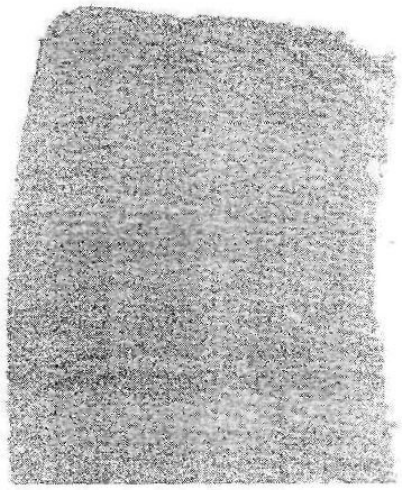

Fig.13 Macrophotograph showing the mode of propagation for the $3TiO_2 + 4Al + 3C$ reaction to produce TiC/Al_2O_3 composites

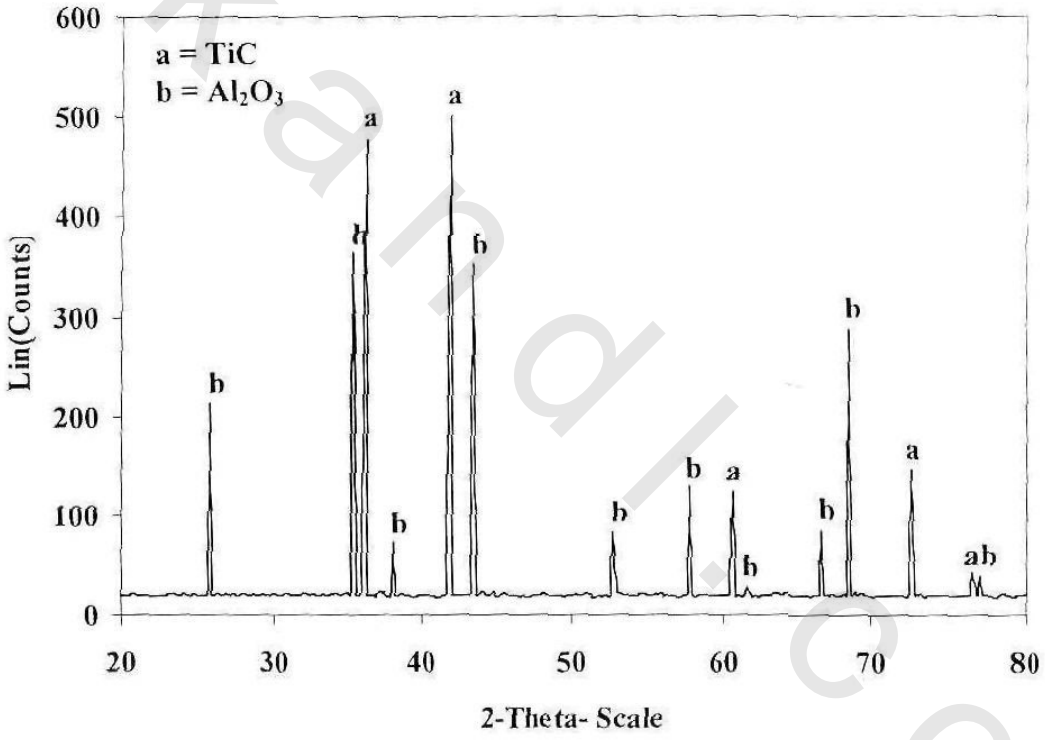

Fig. 14 XRD of combustion products of $TiO_2 + 4Al + 3C$ reaction

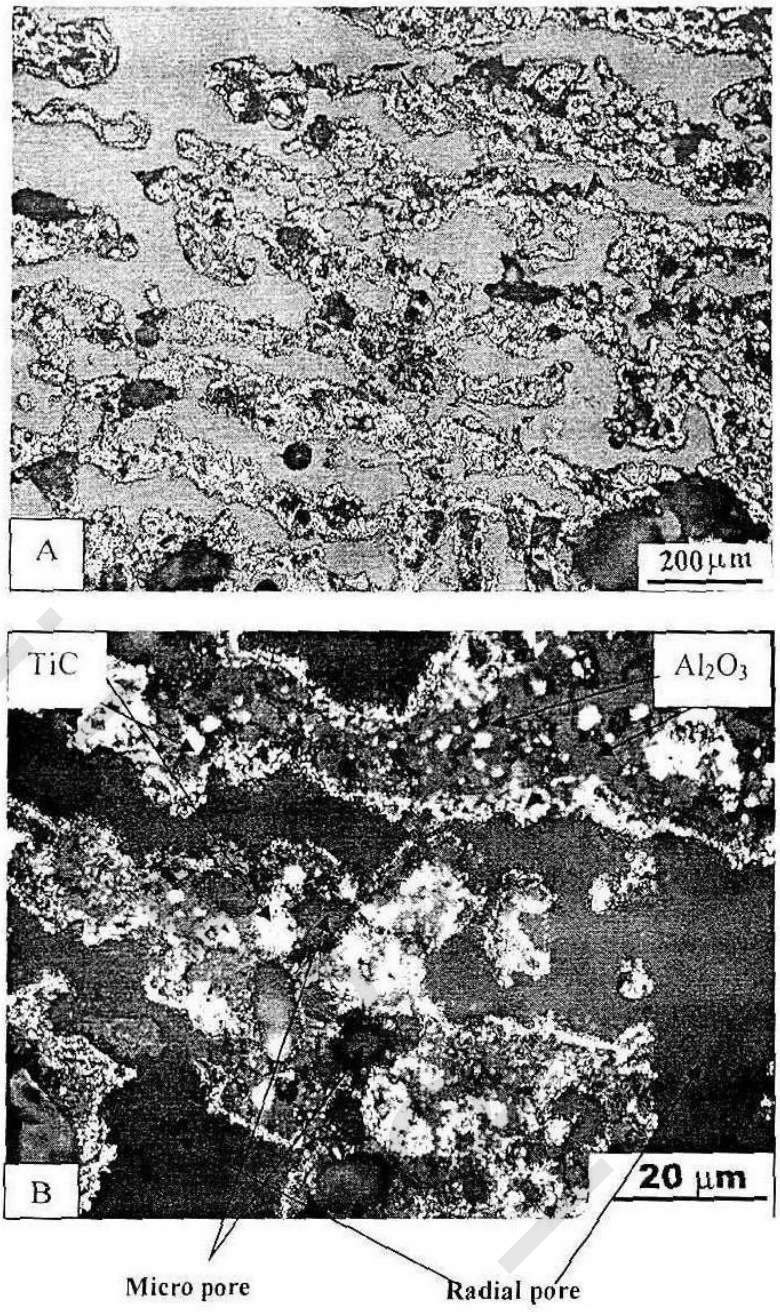

Fig.15 Optical photomicrographs of samples produced from the reaction:

$$3TiO_2 + 4Al + 3C \rightarrow 3TiC + 2Al_2O_3$$

A) Lower magnification;

B) Higher magnification

More over, the colorless phase in Fig.15b is considered to be TiC while the dark phase is Al_2O_3. It can be noticed that the dark phase (Al_2O_3) occupied more volume fraction than the colorless phase (TiC). This can be attributed to the higher density of TiC (4.9 g cm^{-3}) than that of Al_2O_3 (3.97 g cm^{-3}). [119] Also, the percent of Al_2O_3 in the product (53.17 %) is greater than that of TiC (46.83 %).

3.2.3.2 Scanning electron microscopy (SEM)

SEM investigation is conducted to polished horizontal surface coated with gold to ensure good electrical conductivity of the entire components of the sample. Fig. 16 shows the existence of two different phases one is dark and the other is colorless. Energy dispersive spectroscopy (EDS) of the dark phase shows the presence of about 40 % atomic Al and 60 % atomic O which is correspond to Al_2O_3 phase. On the other hand, the colorless phase is composed mainly of titanium and carbon.

It can be seen that the grains of the dark phase are sintered together into a big grain and some of it are disseminated as small particulates into the colorless phase.

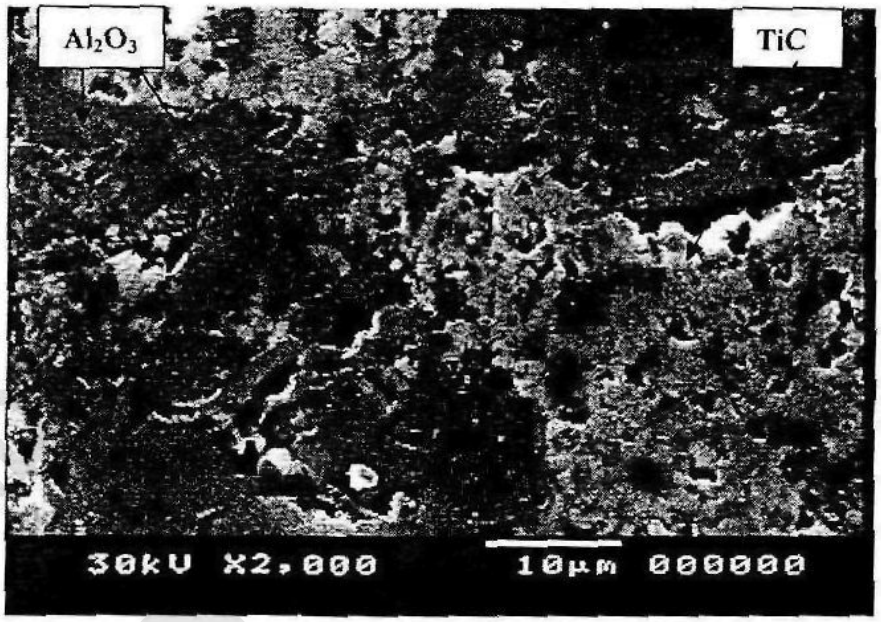

Fig. 16 The SEM micrograph of TiC/Al_2O_3 sample

3.3 Synthesis of TiC/Al_2O_3 composite at different Al grain sizes

In this series of experiments aluminum particle size is varied while the other reactants particle sizes are kept constant. This allowed the individual examination of the effect of aluminum particle size on reaction rate and the microstructure of the synthesized ceramic.

Combustion reaction is conducted at room temperature for five samples containing aluminum powder with different grain sizes (<20, <36, <53, <71, <93 μm). Fig. 17 shows the variation of the combustion wave velocity as a function of aluminum particle size, it can be seen that the wave velocity is inversely proportional to the aluminum grain size. Generally, it decreases with increasing particle size of aluminum, and the reaction fails to propagate at < 93 μm aluminum particle size. In case of larger aluminum partial size, titania and graphite (more fine) form continues phases which envelop the surface of the large aluminum particles. After the reaction, the reaction products (Al_2O_3 and TiC) will deposit on the surface of the molten aluminum sphere and prevents its contact with other reactants. No significant change in the combustion temperature was noticed with increasing the grain size of Al as in Fig. 18.

On the other hand, it is noticed that the aluminum grain size influences the produced microstructure of the products as in Fig. 19. It is observed that the microstructure of the samples containing aluminum particle sizes < 71 μm and < 63 μm are composed of two separate phases (dark and colorless), where the dark phase forms bigger grain than the colorless phase. Alternatively, microstructure of the sample having aluminum particle size < 20 μm forms more homogeneous structure with interpenetrating phases of the colorless and dark constituents.

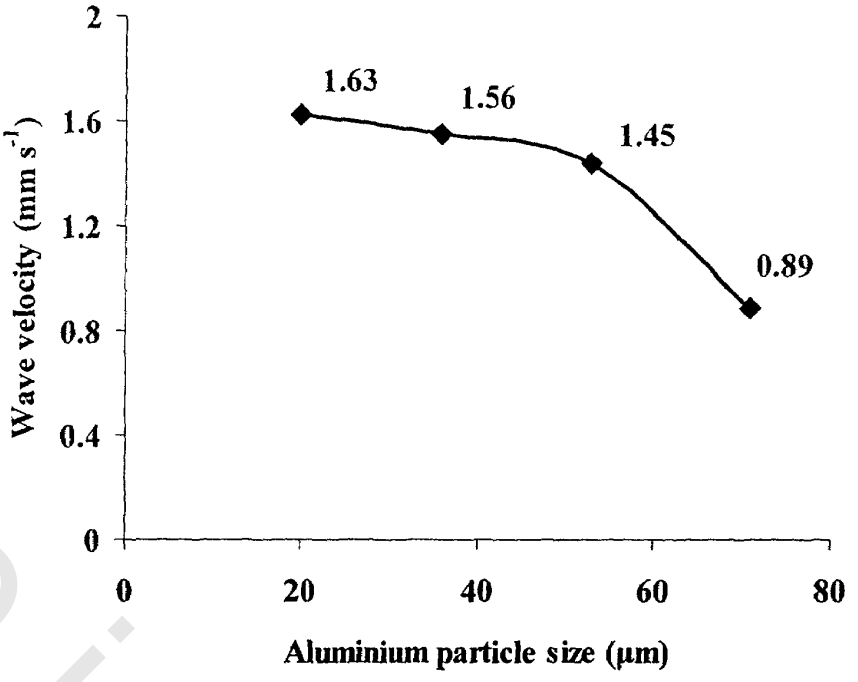

Fig. 17 Effect of aluminum grain size on wave velocity for $3TiO_2$+ 4Al+ 3C reaction

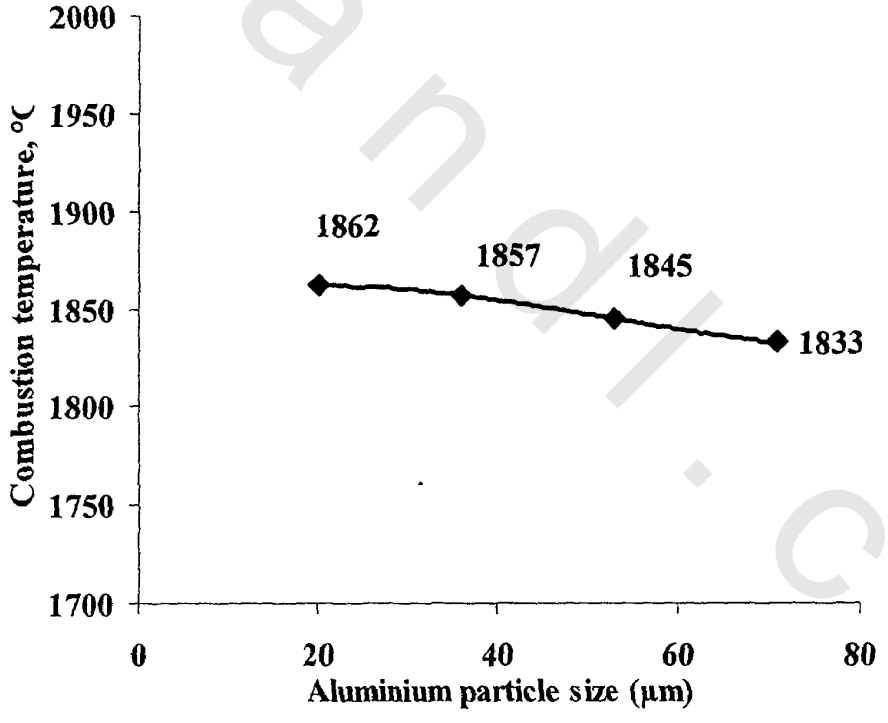

Fig. 18 Effect of aluminum grain size on the measured combustion temperature for $3TiO_2$+ 4Al+ 3C reaction

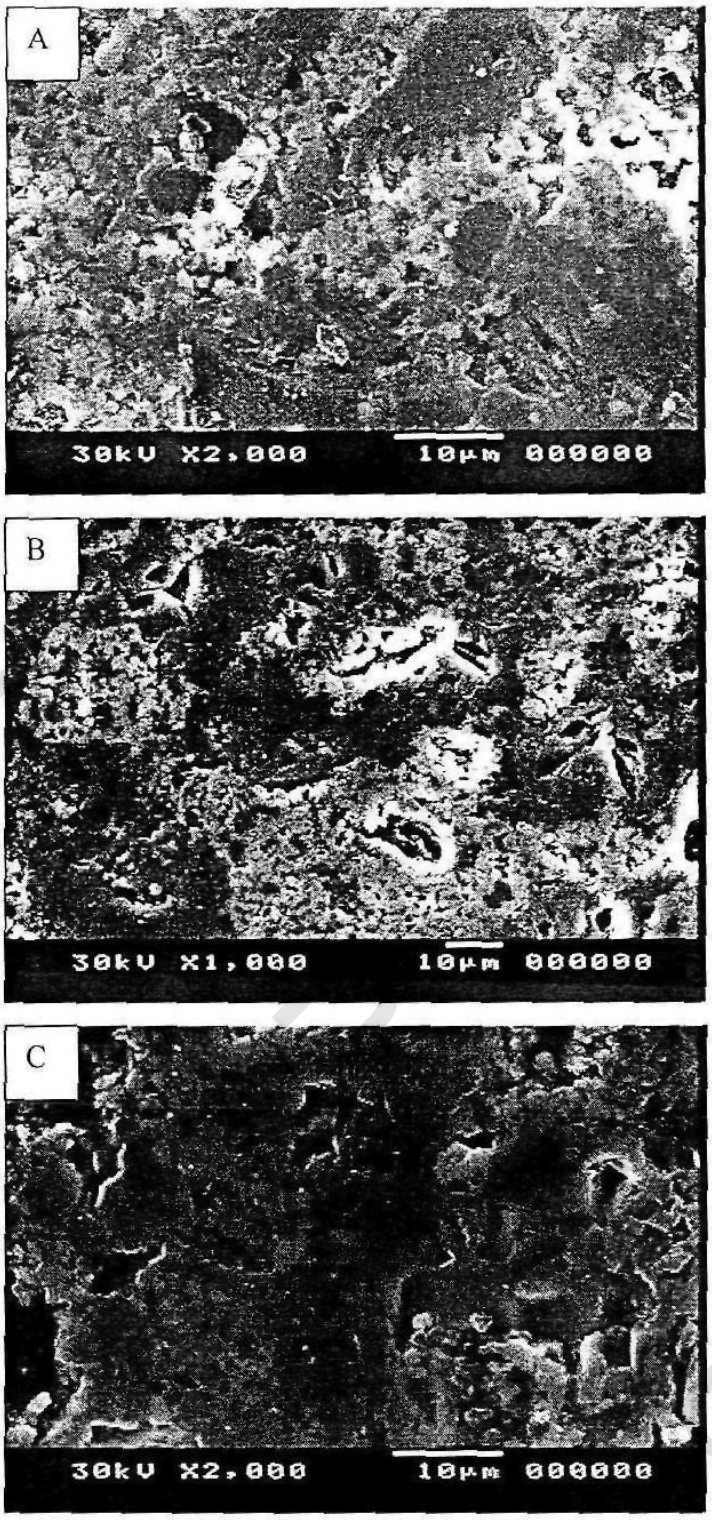

Fig. 19 SEM micrograph of three products samples containing different grain sizes of aluminum metal powder:

A. Particle size less than 71 µm;

B. particle size less than 36 µm;

C. Particle size less than 20 µm.

3.4 Synthesis of TiC/Al_2O_3 composite at different Al additions

One of the main disadvantages of combustion synthesis of ceramic and composite materials is the relatively high levels of porosity, e.g., ≥45 %, present in the product. This factor discusses a novel application of combustion synthesis for producing ceramic-metal composite with reduced levels of porosity by allowing an excess amount of liquid metal, generated by the exothermic reaction, to infiltrate the pores. On the other hand, this application used to control the SHS reaction by lowering the adiabatic combustion temperature. This application of combustion synthesis of ceramic-metal composite materials is discussed with respect to a model reaction system that utilizes an inexpensive oxide, i.e., TiO_2, reacted with carbon and an excess stoichiometric amount of aluminum.

Aluminum metal powder of less than 36 μm particle size is mixed with the powder reactants to produce $3TiC/2Al_2O_3/xAl$, according to the following equation:

$$3TiO_2 + (4 + x)\,Al + 3C \rightarrow 3TiC + 2Al_2O_3 + xAl$$

Samples consisting of 4.77 g wt % (x = 1), 8.91 g wt % (x = 2), 12.57 g wt % (x = 3), 15.83 g wt % (x = 4) and 21.38 g wt % (x = 6) excess aluminum are prepared. The experimental measurements of the variation of wave velocity with aluminum content in argon atmosphere are shown in Fig. 20. The wave velocity increases with a small addition of excess aluminum up to (8.91 g wt %, x = 2) and then begins to decrease at higher additions of diluents with the reaction failing to propagate at 21.38 g wt % excess aluminum. The possible reason for the increased combustion wave velocity was thought to be the increased mass diffusion and heat transfer in the presence of a more liquid phase which wets the solids, increasing the contact area. On the other hand, the decreasing in combustion wave velocity is due to reduced volumetric heat generation as will as the reduced mass diffusivity caused by the reduced

temperature in the combustion zone. The reaction failed to be self sustained at 21.383 wt % excess aluminum because of reaching the dilution limit.

The effect of excess aluminum on the relative density (Dr) and porosity (Po) of the product are given in Fig. 21. Increasing the amount of excess aluminum substantially increases the relative density of the ceramic-metal composite product to 68 %, as the ductile Al particles providing compaction among the TiO_2 and C particles and the liquid aluminum infiltrates some of the pores.

XRD of the reaction products detected titanium carbide and aluminum oxide as the main phases in addition to a moderate intensity peaks corresponding to aluminum metal, no peaks where detected for residual reactants, as in Fig. 22.

Microscopic investigation in Fig. 23 is conducted for samples having excess aluminum contents of (x = 2, x = 4). In case of x = 2, it can be seen that extra amount of aluminum can not wet Al_2O_3, where, big grains of alumina appears separately in the structure. On the other hand, collections of typically rounded TiC grains are noticed immersed in the melted aluminum phase. In case of (x = 4), where, more aluminum is present, a homogenous structure of all phases exist together, where, rounded dark and colorless phases are immersed in aluminum phase.

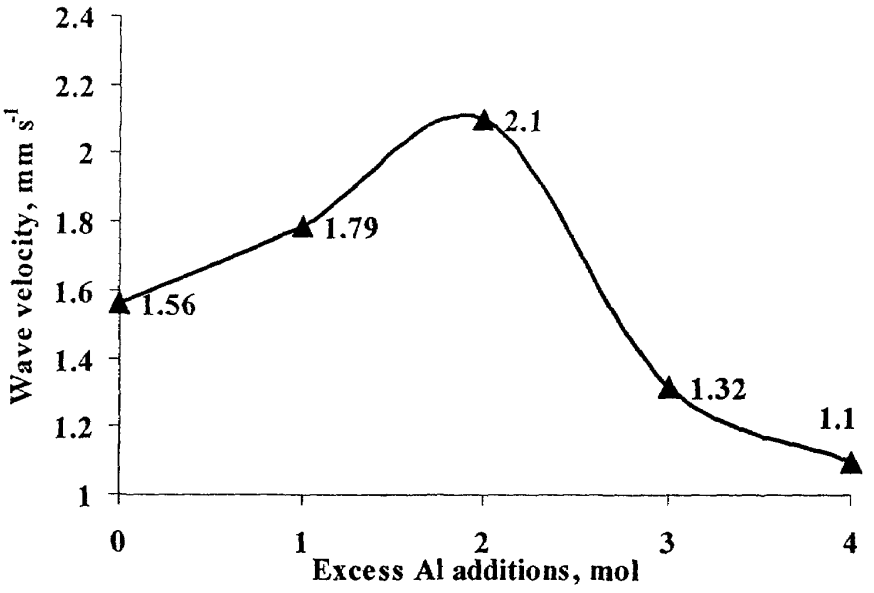

Fig. 20 Effect of excess aluminum additions on the combustion wave velocity of the reaction $3TiO_2$+ 4Al+ 3C

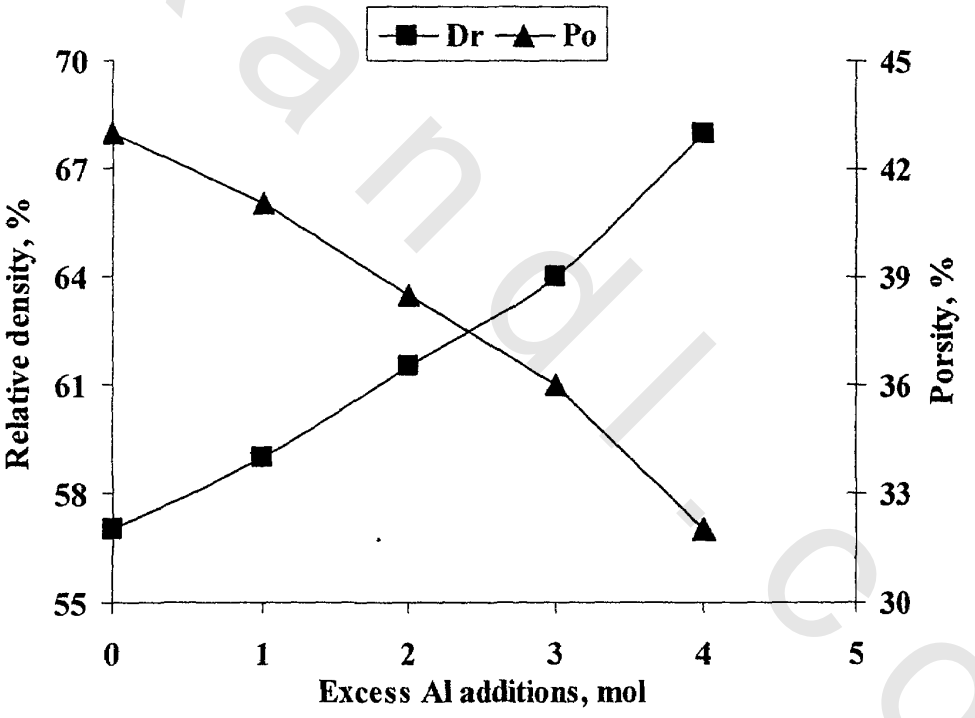

Fig. 21 Effect of excess aluminum additions on the relative density and porosity of the products

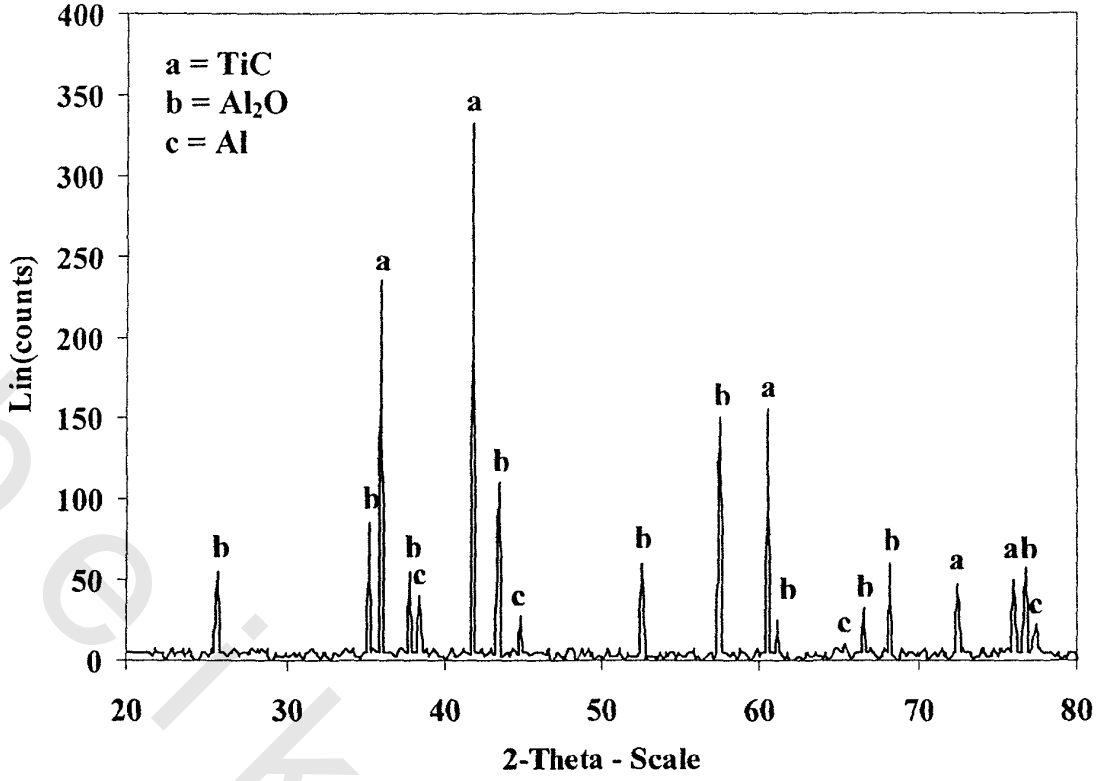

Fig. 22 XRD of combustion product of (TiO_2 + 6Al + 3C) shows the presence of residual reactant aluminum

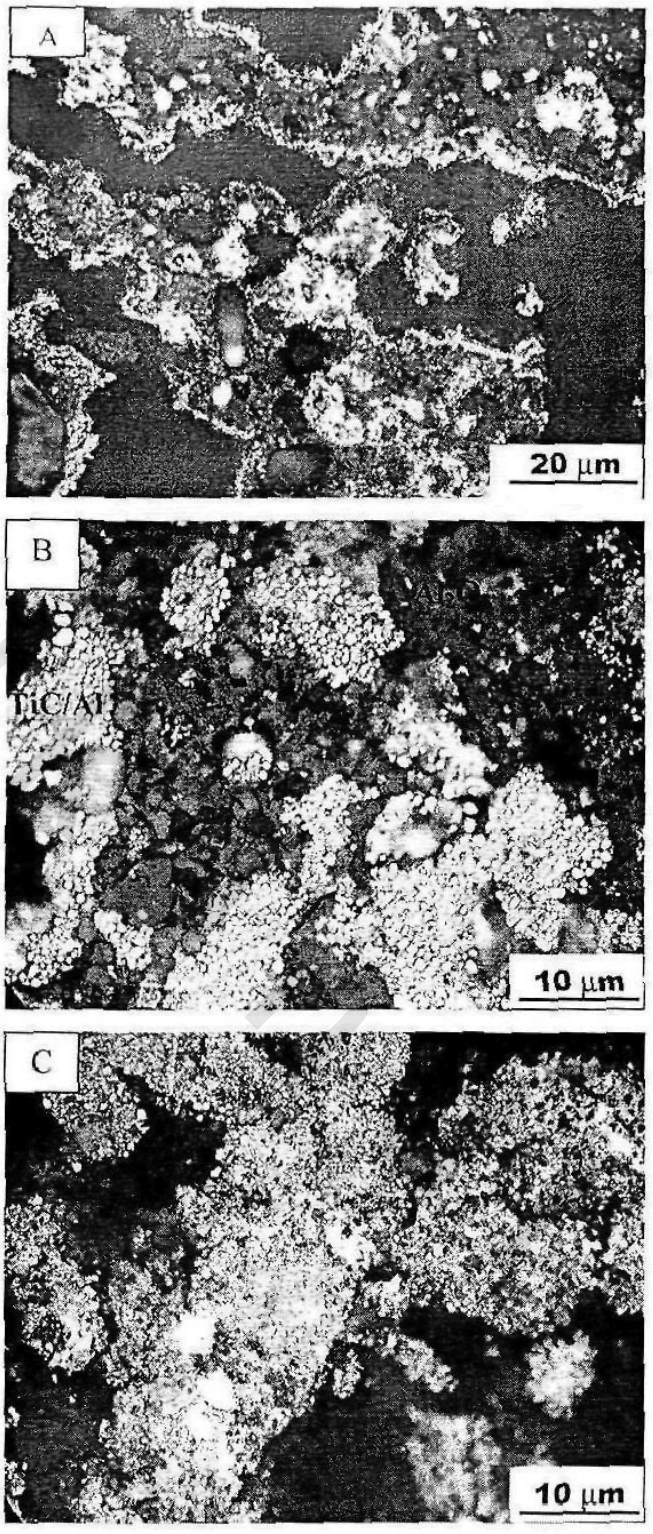

Fig. 23 OM of three products samples containing different amount of aluminum metal powder:

A- $3TiC + 2Al_3O_3$ (x = 0)

B- $3TiC + 2Al_3O_3 + 2Al$ (x = 2, 8.91 g wt %)

C- $3TiC + 2Al_3O_3 + 4Al$ (x = 4, 15.83 g wt %)

3.5 Synthesis of TiC/Al_2O_3 composite at different initial temperatures

Another parameter to control the SHS process is achieved by heating the reactants prior to ignition. When the desired temperature is attained, the sample maintained at that temperature for 25 mints to allow the temperature to equilibrate throughout the reactant compact.

3.5.1 Combustion synthesis of TiC/Al_2O_3 at initial temperature of 192 °C

The temperature of the green specimen is adjusted at 192 °C before ignition and then the combustion reaction is carried out. The resultant temperature profile is depicted in Fig. 24. The *onset* temperature of the thermocouple is changed from the initial temperature 192 °C to 206 °C due to the energy supplied by the igniter. The temperature profile has a maximum combustion temperature of 1887 °C which is achieved after 0.59 s with a temperature rise of 1681 °C. The calculated adiabatic combustion temperature of the reaction at 206 °C is 2260°C. The velocity of the combustion wave still relatively low 1.88 mm s^{-1} as in case of room temperature sample (1.56 mm s^{-1}) and the wave propagation is not steady state where the obtained product has also laminated structure.

The first derivative of the temperature profile is portrayed in Fig. 25, where the maximum heating rate *dT/dt* is 3616 °Cs^{-1}.

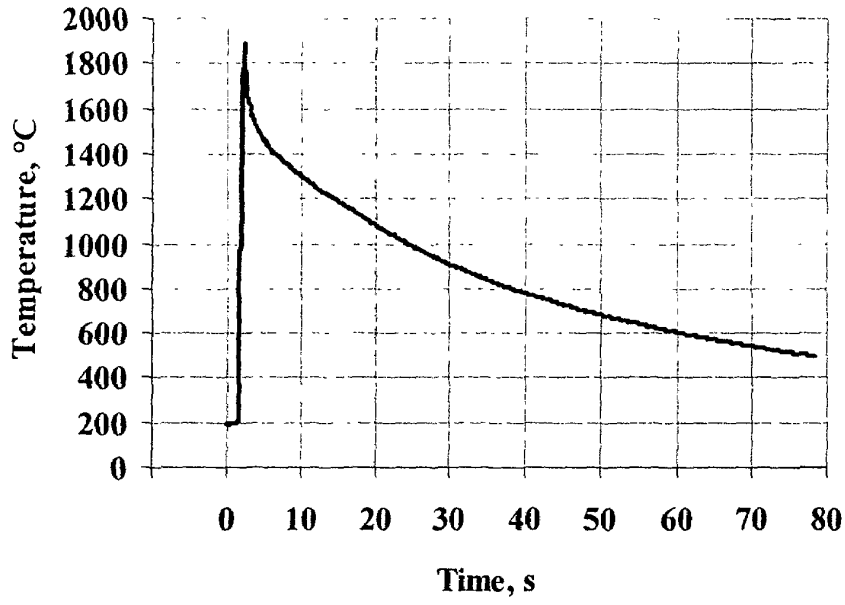

Fig. 24 Temperature profile of the $3TiO_2+4Al+3C$ reaction carried out at 206 °C (*onset*)

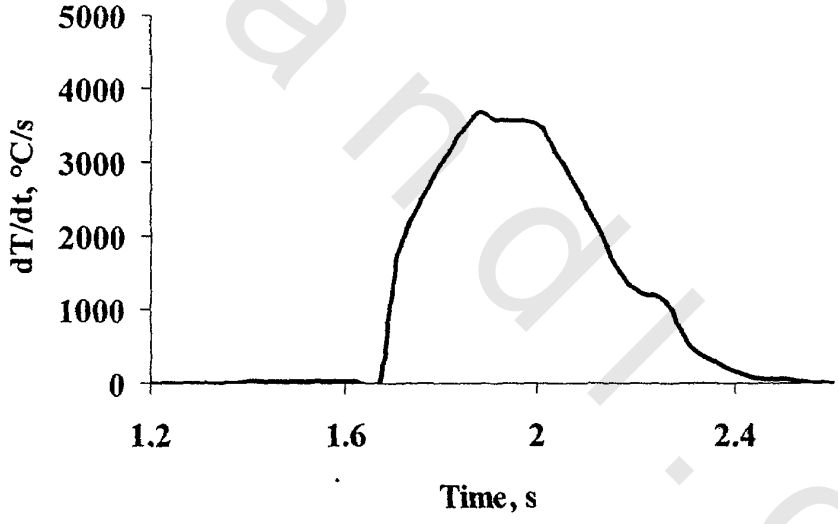

Fig. 25 First derivative of the temperature profile of $3TiO_2+4Al+3C$ reaction carried out at 206 °C (*onset*)

3.5.2 Combustion synthesis of TiC/Al_2O_3 at initial temperature of 299 °C

Fig. 26 shows, the temperature profile of a specimen preheated to 299 °C for 25 min before ignition. The *onset* temperature of the thermocouple is changed from the initial temperature 299 °C to 306 °C due to the energy supplied by the igniter. The temperature profile has a maximum combustion temperature of 1917 °C with temperature rise of 1611 °C. The maximum temperature is reached within 1.5 s. The calculated adiabatic combustion temperature of the reaction at 306 °C is 2339 °C. The measured velocity of the combustion wave is 3.25 mm s^{-1} which is higher than that of the sample ignited at room temperature. The wave propagation is not steady state where the obtained product has also laminated structure.

The first derivative of the temperature profile is described in Fig. 27, where the maximum heating rate *dT/dt* is 4210 °C/s.

3.5.3 Combustion synthesis of TiC/Al_2O_3 at initial temperature of 415 °C

The temperature of the specimen is adjusted at 415 °C before ignition and then the combustion reaction is carried out. The temperature profile is given in Fig. 28. The *onset* temperature of the thermocouple is changed from the initial temperature 415 °C to 430 °C due to the energy supplied by the igniter. The temperature profile has a maximum combustion temperature of 1967 °C with temperature rise of 1537 °C. The temperature of the thermocouple location rose to its maximum value within 1.73s. The calculated adiabatic combustion temperature of the reaction at 430 °C is 2444 °C. The velocity of the combustion wave is 3.84 mm s^{-1} and the wave propagation is not steady state where the obtained product has also laminated structure. The first derivative of the

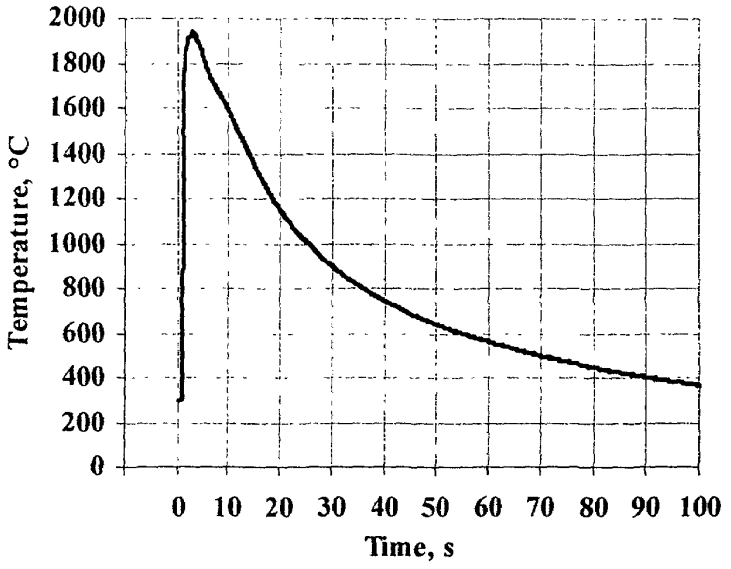

Fig. 26 Temperature profile of the $3TiO_2+4Al+3C$ reaction carried out at 306 °C (*onset*)

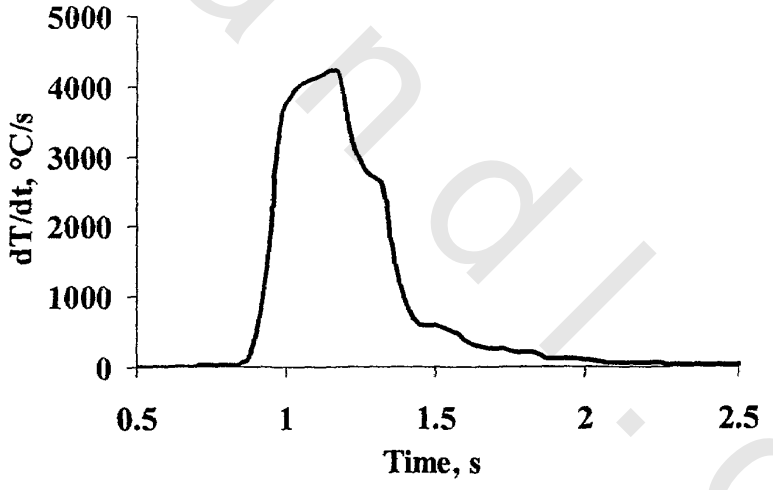

Fig. 27 First derivative of the temperature profile of $3TiO_2+4Al+3C$ reaction carried out at 306 °C (*onset*)

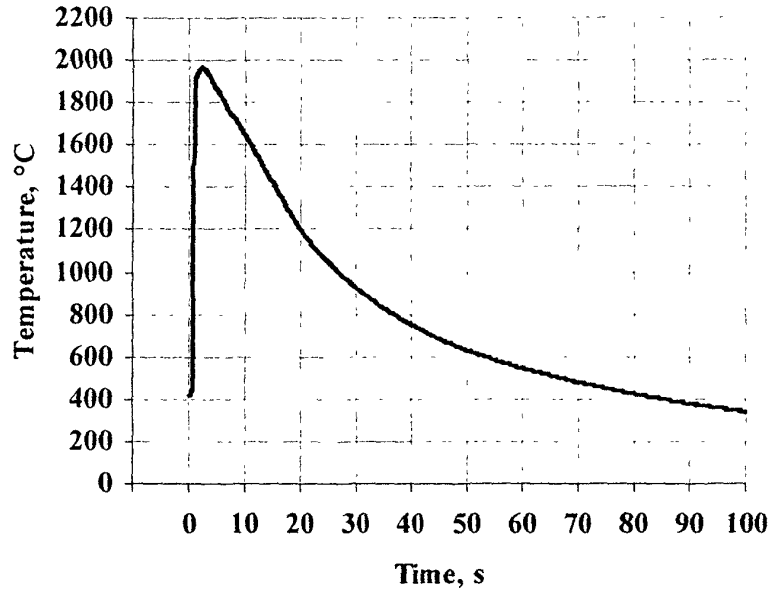

Fig. 28 Temperature profile of the $3TiO_2+4Al+3C$ reaction carried out at 430 °C (*onset*)

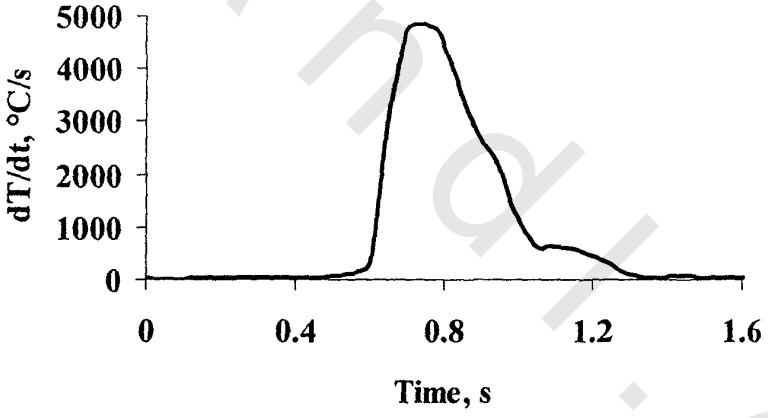

Fig. 29 First derivative of the temperature profile of $3TiO_2+4Al+3C$ reaction carried out at 430 °C (*onset*)

temperature profile is represented in Fig. 29, with the maximum heating rate *dT/dt* of 4860 °C s^{-1}.

3.5.4 Combustion synthesis of TiC/Al_2O_3 at initial temperature of 501 °C

The initial temperature of the green specimen is adjusted at 501 °C before ignition and then the combustion reaction is conducted. The temperature profile is represented in Fig. 30. The *onset* temperature of the thermocouple is shifted from the initial temperature 501 °C to 511 °C due to the energy supplied by the igniter. The temperature profile has a maximum combustion temperature of 2002 °C with temperature rise of 1491 °C. The temperature of the thermocouple rose to its maximum value within 0.55 s. The calculated adiabatic combustion temperature of the reaction at 511 °C is 2512 °C. The velocity of the combustion wave is 4.67 mm s^{-1} and the wave propagation is not steady state where the obtained product has also laminated structure.

The first derivative of the temperature profile is shown in Fig. 31, where the maximum heating rate *dT/dt* is 5227 °Cs^{-1}.

3.5.5 Combustion synthesis of TiC/Al_2O_3 at initial temperature of 597 °C

The temperature of the green sample is adjusted at 597 °C before ignition and then the combustion reaction is carried out. The resultant temperature profile is described in Fig. 32. The onset temperature of the thermocouple is altered from the initial temperature 597 °C to 600 °C as a result of the energy supplied by the igniter. The temperature profile has a maximum combustion temperature of 2179 °C with temperature rise of 1579 °C. The temperature of the thermocouple rose to its maximum value within 0.61 s. The calculated adiabatic combustion temperature of the

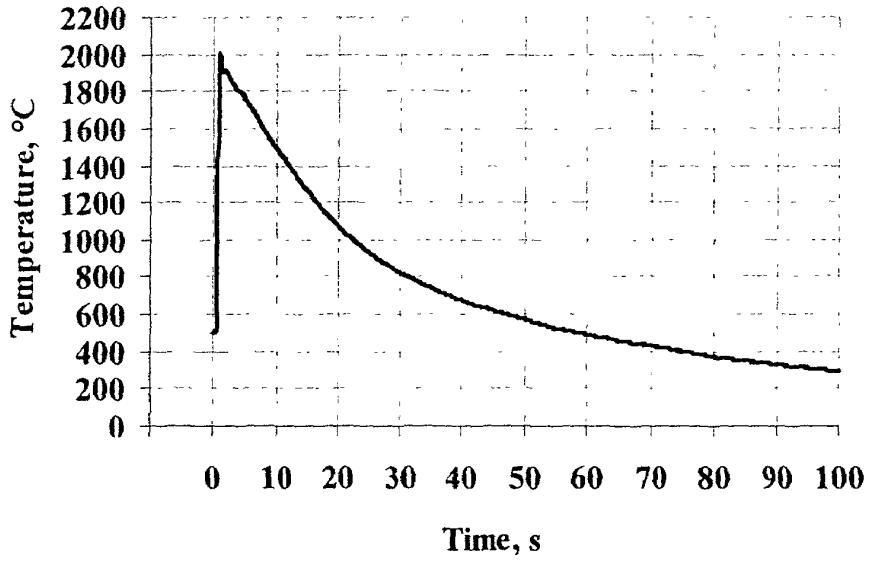

Fig. 30 Temperature profile of the $3TiO_2+4Al+3C$ reaction carried out at 511 °C (*onset*)

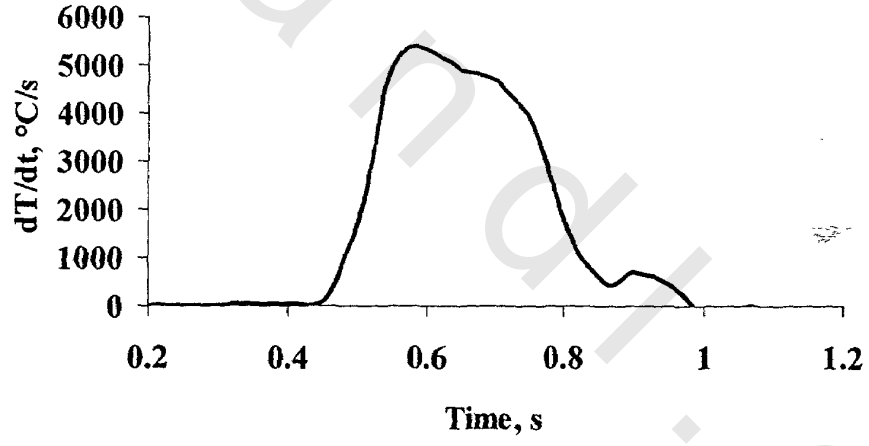

Fig. 31 First derivative of the temperature profile of $3TiO_2+4Al+3C$ reaction carried out at 511 °C (*onset*)

reaction at 600 °C is 2584 °C. The velocity of the combustion wave is high 5.99 mm s^{-1} and the wave propagation is not steady state where the obtained product has also laminated structure.

The heating rate of the temperature profile is illustrated in Fig. 33, where the maximum heating rate *dT/dt* is 5644 °Cs^{-1}.

From the aforementioned discussion it is noticed that **the combustion wave velocity** increases from 1.56 to 5.99 mm s^{-1} with increasing the preheating temperature from room temperature to 597 °C, Fig. 34. This is because of increasing the preheating temperature which contributes more energy to the system and brings it more rapidly to its ignition temperature and smoothes the propagation of the wave from one layer to another.

Also, **the measured combustion temperature** is related to the initial temperature, therefore, it increased from 1857 to 2179 °C as the initial temperature increased from room temperature to 597 °C, Fig. 35.

This can be explained as follows; in addition to the heat released from combustion reaction, each spot in the reaction medium has three other sources of heat energy which cause temperature rising. **The first** source comes from the approach of the wave, **the second** source form the igniter, and **the last** one from preheating the reaction medium. The quantity of energy at a given point in the system is simply the summation of all the above energies. So, raising the initial temperature of the reaction medium supplies the system with additional amount of heat, which in turn increases the total amount of heat of the reactants and finally, the combustion reaction temperature increases.

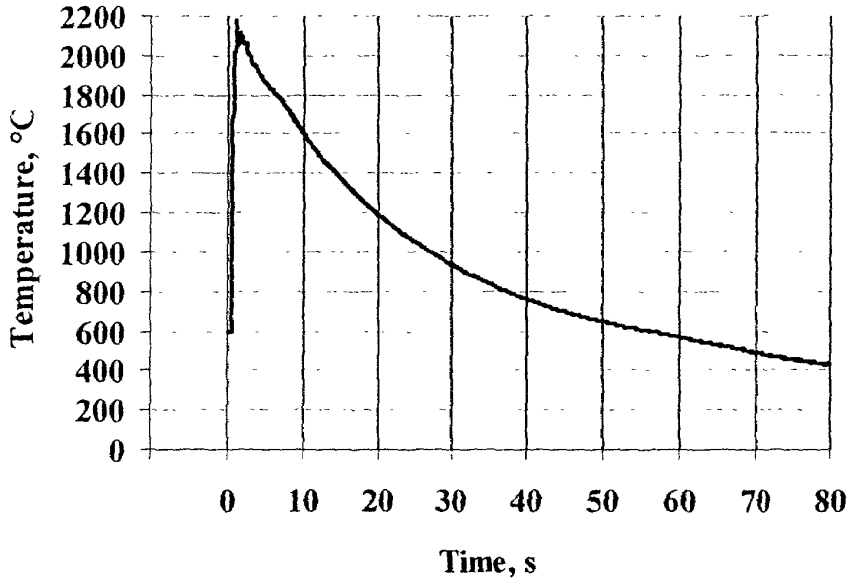

Fig. 32 Temperature profile of the $3TiO_2+4Al+3C$ reaction carried out at 600 °C (*onset*)

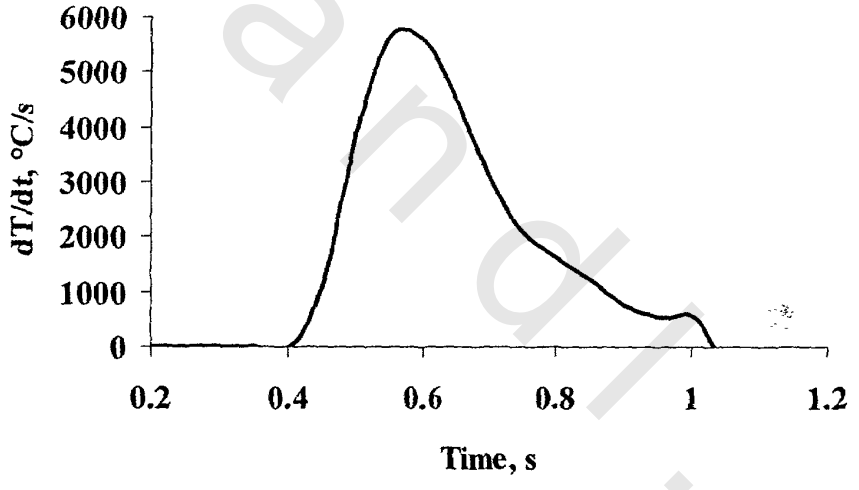

Fig. 33 First derivative of the temperature profile of $3TiO_2+4Al+3C$ reaction carried out at 600 °C (*onset*)

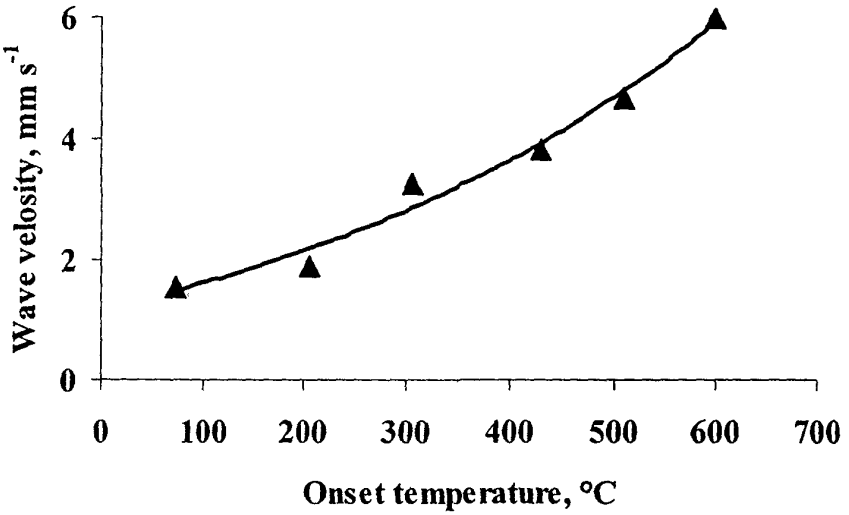

Fig. 34 Effect of preheating temperature (*onset*) on combustion wave velocity

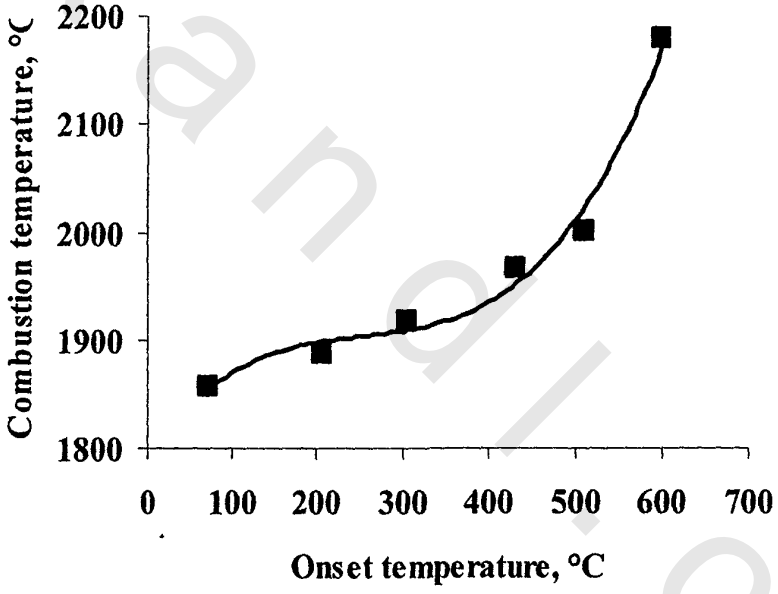

Fig. 35 Effect of preheating temperature (onset) on combustion temperature

X- ray diffraction (XRD) confirmed that reaction at all different initial temperatures proceeded to completion, TiC and Al_2O_3 peaks were present, and no peaks corresponding to the starting materials were observed as shown in Fig. 36.

Also, it can be noticed from Fig. 37 that **the maximum heating rates** considerably increases with increasing the initial temperatures.

Scanning electron microscopic investigation (SEM) of the combustion products synthesized at different initial temperatures in Fig. 38 shows that as the initial temperature increases, the two phases (dark and colorless) tend to form something like a matrix and reinforcement where the dark phase is the matrix and the colorless phase is the reinforcement which is disseminated in the matrix. The dark phase (Al_2O_3) seems to be more sintered with increasing the initial temperature. This is due to the combustion temperature is elevated with increasing the initial temperature and become much more than the melting point of Al_2O_3 (2053 °C), as shown in Table 4

Table: 4 Adiabatic and combustion temperature for reactions carried out at different initial temperatures

Selected sample	T_i °C	T_c °C	T_{ad} °C
A	Room temp.	1857	2371
B	415	1967	2717
C	597	2179	2800

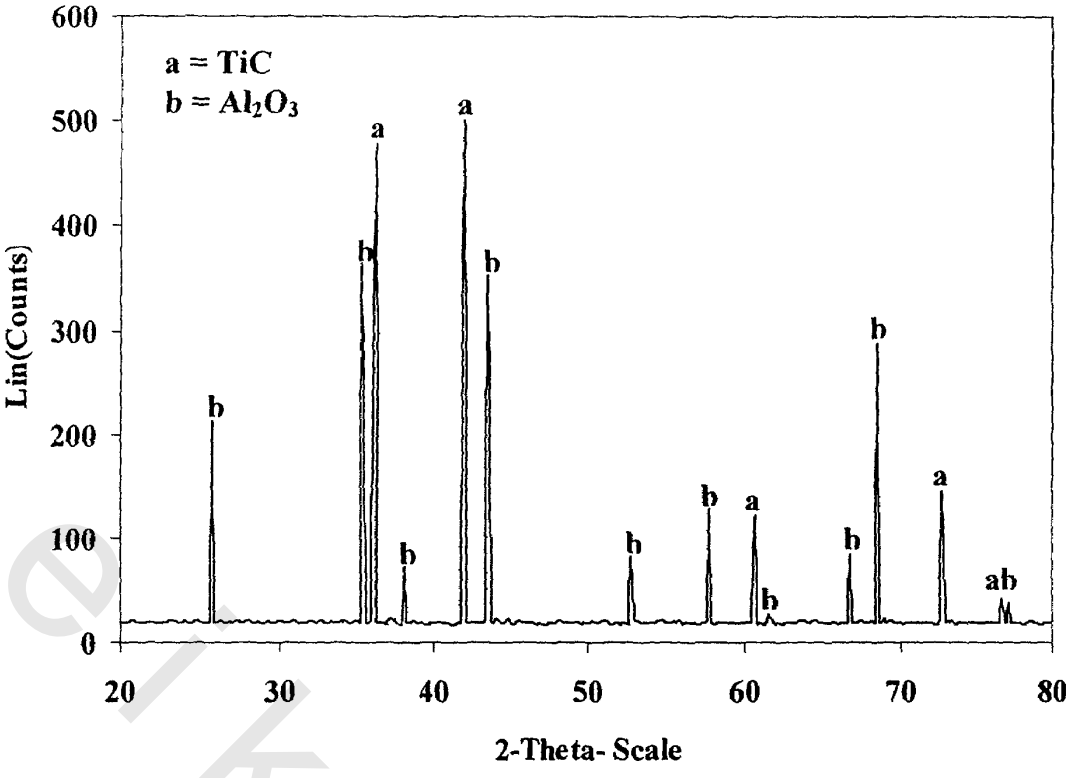

Fig. 36 XRD for obtained product carried out at 415 °C

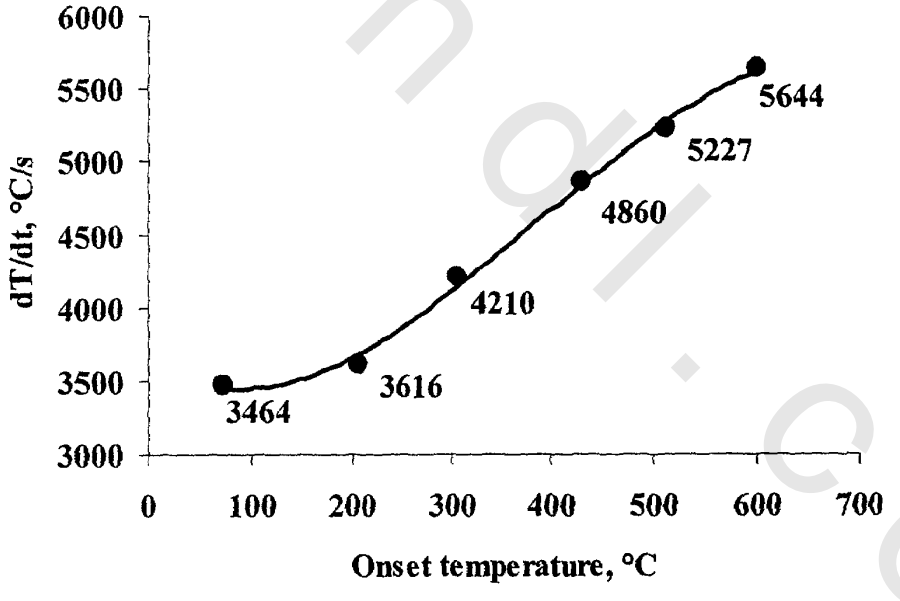

Fig. 37 Variation of the heating rate with onset temperature

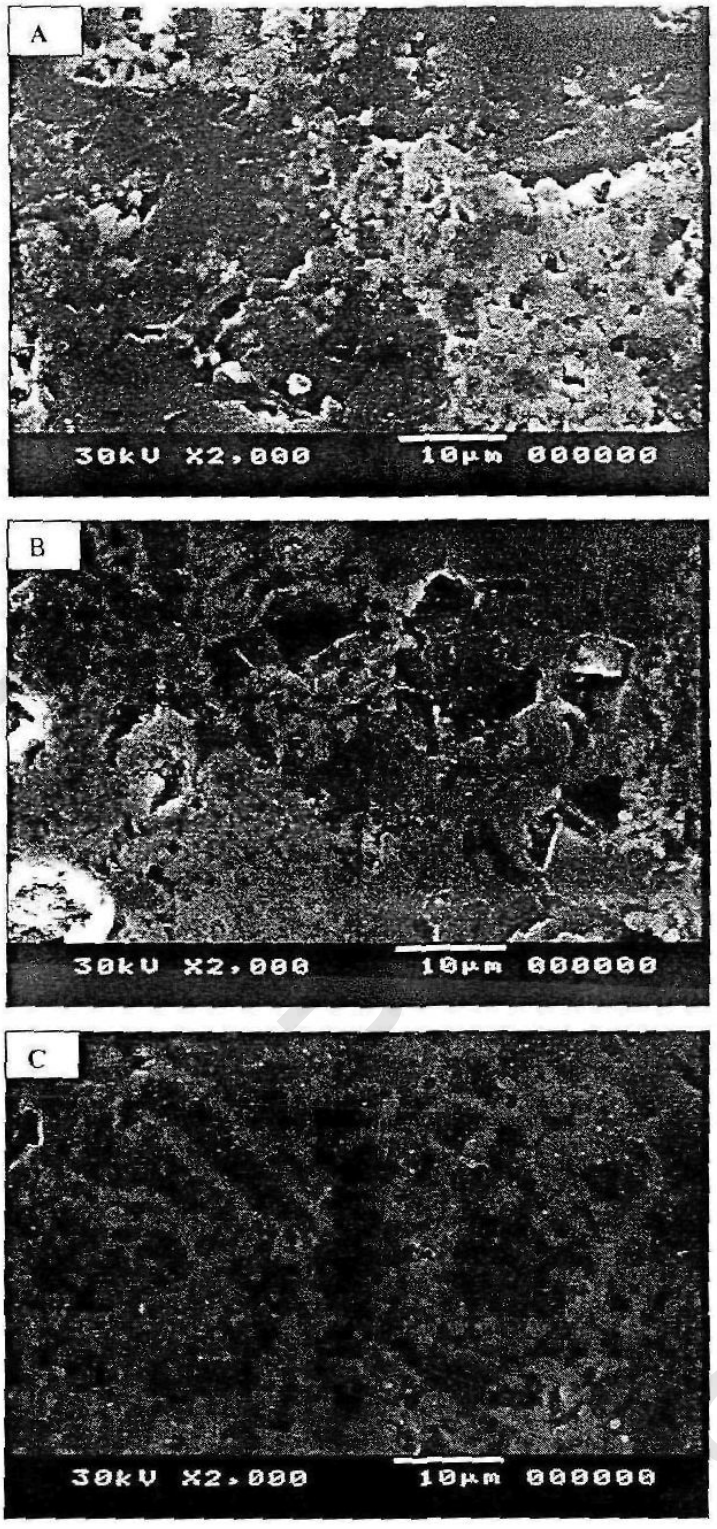

Fig. 38 SEM micrograph of three products samples carried out at different initial temperatures:

A- At room temperature

B- At 415 °C

C- At 597 °C

3.6 Oxidation behavior of porous product

Oxidation tests are carried out in heated muffle furnace up to 800°C for three hours in open air. The samples are separately put in a platin crucible. To understand the oxidation behavior of TiC/Al_2O_3 porous product (porosity 68 %) at different temperatures, the samples after a three hours oxidation are characterized from phase identification by XRD analysis.

Before 400 °C, XRD consists only of the diffraction patterns of TiC and Al_2O_3 with no indication for formation of any titanium oxides. At 400 °C the oxidation of TiC starts where small intensity peaks corresponding to lower oxide of titanium (Ti_4O_7) is detected, Fig. 39. However, at 600 °C, small peaks corresponding to TiO_2 are identified besides very weak peaks of Ti_4O_7. The intensities of the lines corresponding to TiO_2 increase while those of the Ti_4O_7 decrease with increasing the temperature from 600 to 800 °C, Fig. 40, 41. At 800 °C the Ti_4O_7 diffraction pattern is not detected, Fig. 42.

These results suggest that this material should avoid being directly exposed to air above 400 °C.

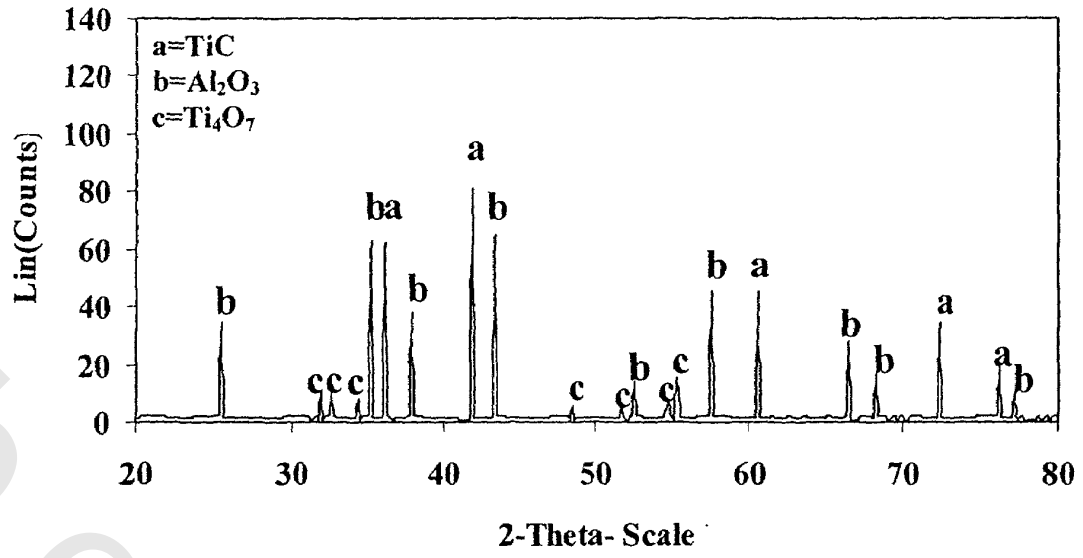

Fig. 39 XRD patterns of TiC/Al_2O_3 porous composite oxidized at 400°C in air for three hrs.

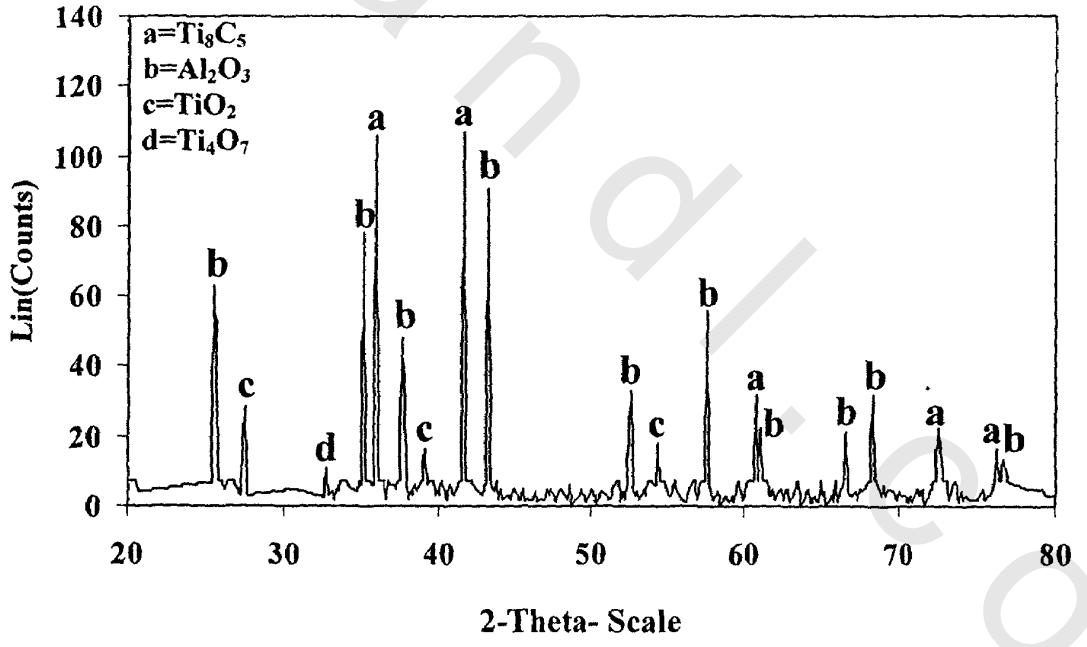

Fig. 40 XRD patterns of TiC/Al_2O_3 porous composite oxidized at 600°C in air for three hrs.

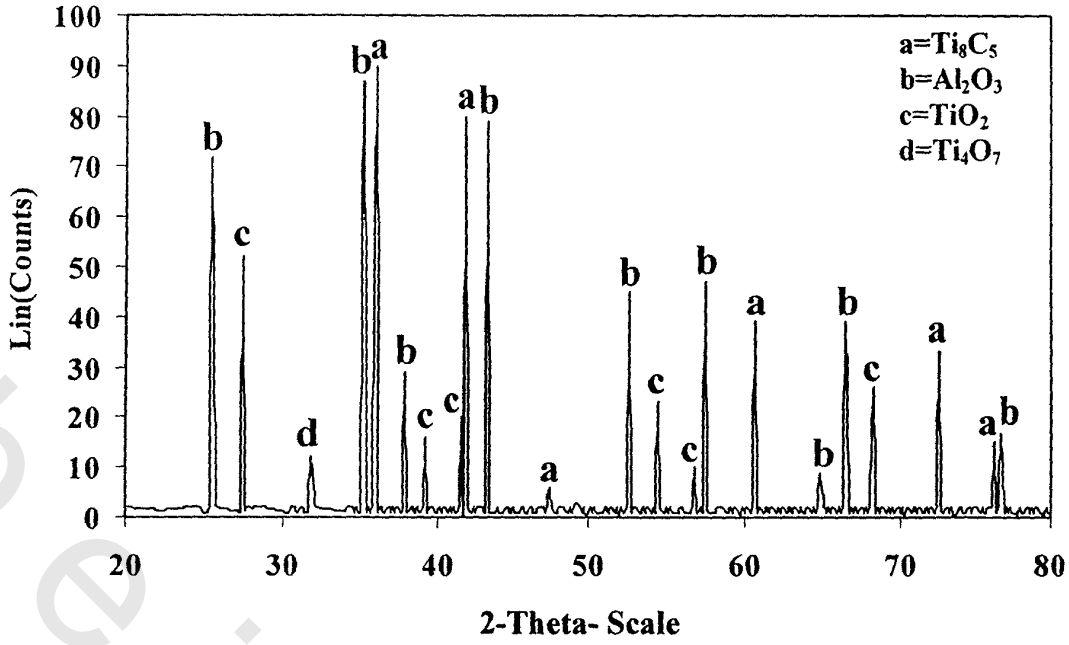

Fig. 41 XRD patterns of TiC/Al_2O_3 porous composite oxidized at 700°C in air for three hrs.

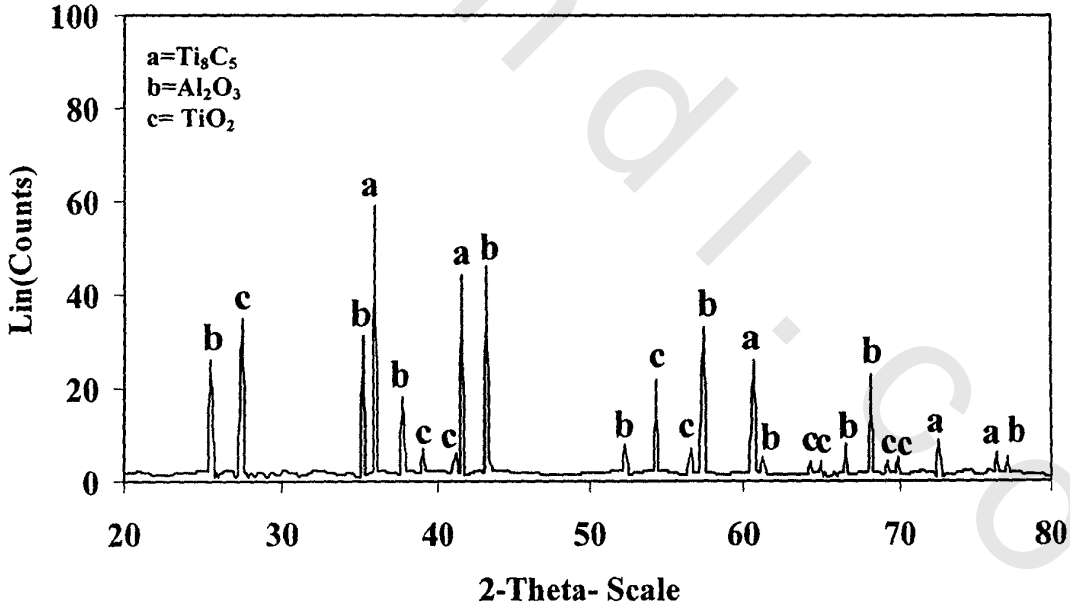

Fig. 42 XRD patterns of TiC/Al_2O_3 porous composite oxidized at 800°C in air for three hrs.

3.7 Kinetic study for the combustion synthesis of TiC/Al_2O_3

Activation energy calculations

Kinetic investigations in self-propagating combustion synthesis reactions have primarily utilized two experimental approaches: combustion wave velocity measurements and temperature profile determinations. In the former the temperature dependence of the wave velocity is used to calculate the activation energy of the process and in the latter the reaction rate is used to determine the same kinetic term. In this work the first method will be applied.

Wave velocity method

According to the following equation [19]:

$$\mathbf{u}^2 = [f(n)^a k_o C_p R T_c^2] / [QE \cdot \exp(-E/RT_c)],$$

the main parameters necessary to calculate the activation energy E (the wave velocity u and the maximum combustion temperature T_c) are measured experimentally from several $3TiO_2 + 4AL+3C$ reactions which carried out at different onset temperatures. So by increasing the initial temperature of the specimen, both the wave velocity and the combustion temperature increase too. The values obtained at various onset temperatures under argon atmosphere are contained in table 5.

From the above data, $\log (u/T_c)$ and $10^4/T_c$ are plotted against each other, Fig. 43. The slopes of the obtained straight lines = $\partial \log (u/T_c)/ \partial(10^4/T_c)$ are evaluated where the activation energy $E = -2 \times 2.303\ R \times 10^4 \times$ slope, $Jmol^{-1}$. Depending on the above data the activation energy of the $3TiO_2 + 4AL+3C$ reaction are calculated and equal to 316.35 kJ/mol. In order to calculate the activation energy in case of adiabatic condition, the same procedure is repeated by using the calculated adiabatic combustion temperature instead of the measured combustion temperature. The obtained results are given in Table 6 and Fig. 44. The determined

activation energy in case of adiabatic condition equals 348.34 $kJmol^{-1}$, which is higher than that in case of non-adiabatic condition.

Table: 5 Onset temperatures and the corresponding measured wave velocities and combustion temperatures for $3TiO_2 + 4AL+3C$ system

T_i, °C	u (mm/s)	T_c °C	Tc+273 °K	$10^4/T_c$	$\log(u/T_c)$
73	1.5552	1857	2130	4.694835681	-3.1366
206	1.883	1887	2160	4.62962963	-3.0596
306	3.255	1917	2190	4.566210046	-2.8279
430	3.84	1967	2240	4.464285714	-2.7659
515	4.666	2002	2275	4.395604396	-2.688
600	5.999	2179	2452	4.078303426	-2.6114

Table: 6 Onset temperatures and its corresponding adiabatic temperatures and the measured wave velocities for $3TiO_2 + 4AL+3C$ system

T_i, °C	u (mm/s)	T_{ad} °C	T_{ad}, K	$10^4/T_{ad}$	$\log(u/T_{ad})$
73	1.5552	2162.34	2435.34	4.10620283	-3.1948
206	1.883	2260.27	2533.27	3.947467108	-3.1288
306	3.255	2339.38	2612.38	3.827927024	-2.9045
430	3.84	2444.25	2717.25	3.68019137	-2.8498
515	4.666	2511.95	2784.95	3.590728738	-2.7759
600	5.999	2583.77	2856.77	3.50045681	-2.6778

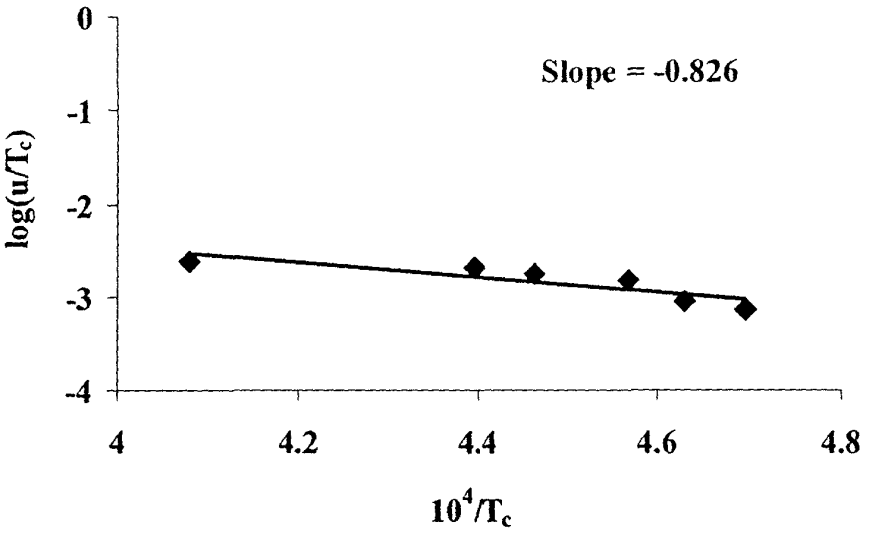

Fig. 43 Arrhenious plots for the wave velocity analysis of $3TiO_2$ + 4AL+3C reaction, In case of no adiabatic conditions

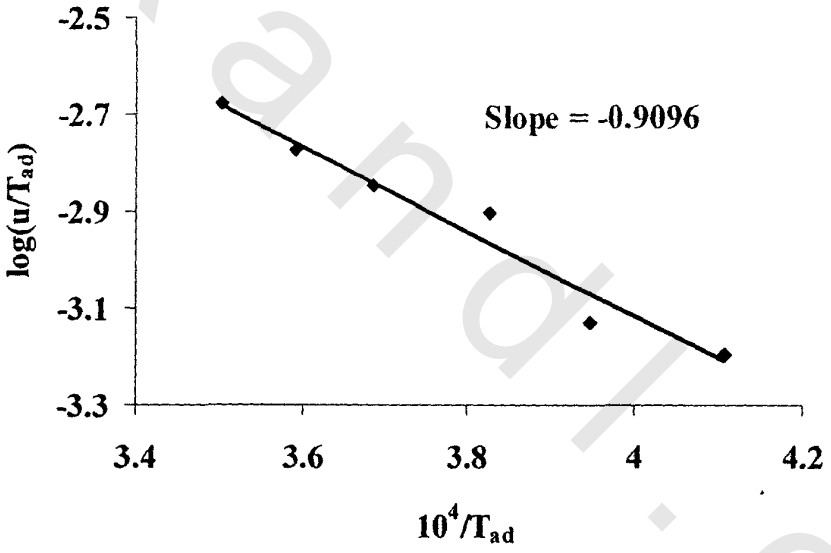

Fig.44 Arrhenious plots for the wave velocity analysis of reaction in case of adiabatic conditions

Future work

During this work titanium carbide/aluminum oxide composites are successfully synthesized in their powder form.

For These composites to be applicable we recommend that

- Further research efforts showed are done in filed of sintering such material at high temperature and pressure in order to increase their density to form dense materials.
- Enhancing mechanical properties of TiC/Al_2O_3 and increase their ductility by blending these materials with other metals such as: Cupper, Nickel, Iron and Magnesium.